International Journal of Engineering (IJE)
Singaporean Journal of Scientific Research(SJSR)
Vol.6.No.6.2014 Pp.284-288
Available at:www.iaaet.org/sjsr
Paper Received:19-09-2014
Paper Accepted:05-10-2014
Paper Reviewed by:1Prof.Dr.Karthikeyan2. Chai ChengYue

AN ISOLATED BOOST RESONANT CONVERTER FOR PHOTOVOLTAIC APPLICATIONS

Jing-song Li, Hai-yan Yu and Xiao-guang Zhang
Zhejiang University,
China

ABSTRACT

Effective photovoltaic power conditioning requires efficient power conversion and accurate maximum power point tracking to counteract the effects of panel mismatch, shading, and general variance in power output during a daily cycle. In this paper, in this paper, a boost resonant converter is proposed withlow component count, galvanic isolation, simple control, as well as high efficiency across a wide input and load range.

Key words: PV,MPPT.,

I. INTRODUCTION

Power conversion for photovoltaic (PV) applications, as opposed to more conventionalconverter configuration requires system that is capable of responding to a wide range of input voltage and current conditions. PV voltage varies with panel construction and operating temperature, while the PV current changes largely due to solar irradiance and shading conditions [1].If a converter is designed only for high peak efficiency, the conditions common for many PV installations will force the converter into another operating region where it is much less efficient. So power conditioning system (PCS) is introduced in order to improve the efficiency called, weighted efficiency through an average day [2], [3]. Also in the photovoltaic system, power conditioning system design process is necessary for galvanic isolation between the PV panel and the electric utility system. While an ungrounded, grid-connected PV array is permitted by many electriccodes, galvanic isolation can be preferred for various reasons. With thisvoltage boost ratio is improved and ground leakage current is reduced. Thus overall safety during the fault conditions is improved [4]-[6].Maximum power point tracking (MPPT) can achieve more energy than the centralized system [7]. Some authors have also proved that a system structure with the PV panels connected in parallel can be much more efficient in low-light and partially shaded conditions than a series -connected system.These leads to make the single-panel PV micro inverter (dc-ac), or an isolated microconverter (dc-dc),for performance -based analysis. In either system, the dc-dc stage implements MPPT optimization, while the second stage attempts to regulate the dc-link voltage by sending power to the utility grid. Block diagrams showing the micro inverter and micro converter are provided in fig.1.It is this combination of high efficiency, galvanic

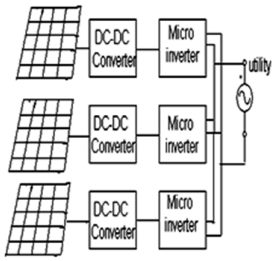

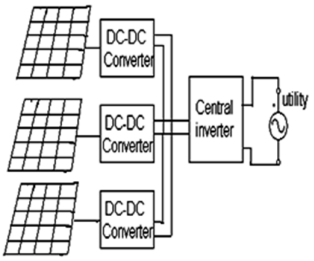

(a) (b)

Fig.1. Distributed (a) micro inverter and (b) microconverter system structures.

Isolation, and a localized, distributed approach to energy conversion that has prompted the proceeding technical development.

II. PROPOSED CONVERTER

The concept of using DC transformer in the proposed system requires an additional element to provideregulation capability. The method proposed in this paper provides a traditional boost converter element which integrates DC transformer with only the addition of a single inductor. The design of the converter is simple and can be controlled using simple fixed frequency pulse width modulation. Thediscrepancies can be found on the maximum and minimum duty cycle. For PV applications, this circuit provides galvanic isolation, low switching loss (Zero Current Switching is achieved through output diodes), low circulating energy, as well as simple gate drive and control .in the following sections will discuss the synthesis of the topology, key waveforms and operational characteristics design procedures well as experimental results.

III. CONVERTER SYNTHESIS

When considering the series-resonant DCX as part of this new hybrid circuit, it is important to notice the half-wave res-onant behavior by which it operates. During the on-period of either switch a resonant circuit is formed by a combination of the input-side capacitors, the output-side capacitors, and the transformer leakage inductance. The unidirectional nature of the output diodes prevents this circuit from resonating perpetually, and instead, only a resonant period consisting of one half-sine wave is visible. Provided that this resonant period is allowed to complete fully before the primary-side switches change states, the series-resonant circuit is naturally soft-switching on both turn-on and turn-off (ZVS and ZCS). If both resonant periods are allowed to fully complete, the system has no method by which to regulate theoutput, and the output is simply a reflection of the input. Hence, the necessary addition of another "regulating element," in this case a boost converter, is shown in Fig. 2.The boost converter regulates the effective input voltage to the series-resonant converter, allowing it to run as a DCX with high efficiency. The cost is two additional transistors, with their associated gate drive requirements, and some additional switching and conduction loss.

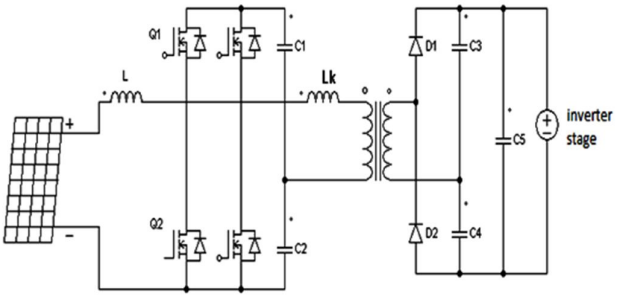

Fig2. Resonant half-bridge with separate boost input stage.

This circuit may be further simplified by integrating the system so that the boost converter function is implemented by the original two MOSFETs. A straightforward method to understand this is to directly tie the input inductor to the midpoints of both active switching legs simultaneously. Note that this change directly ties the inductor to one terminal of the transformer. This additional connection renders the upper MOSFETs (Q_X and Q_1) as well as the lower MOSFETs (Q_Y and Q_2)in parallel, so long as their switching patterns are synchronized. Thus, the circuit may be simplified, with the additional connection and the removal of Q_X and Q_Y, into the topology shown in Fig. 3.Because the now single upper and lower FETs (Q_1 and Q_2) is effectively replacing two parallel

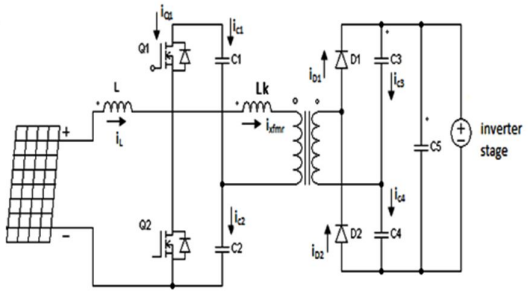

Fig 3: IBR Converter.

FETs, they carry the combined current from the original four switches. Also, as long as the resonant behavior is allowed tocomplete, the output diodes, D_1 and D_2, still achieve ZCS. This particular circuit topology is similar to that of the "boost half-bridge".(BHB); however, the actual operation of this circuit is quite different.In the BHB, the operating currents are that of the hard-switching half-bridge, giving the converter a poor power factor at the transformer. This makes it difficult for the converter to achieve a wide range ofoperation, even with ZVS. Also, the voltageTransfer ratio is highly nonlinear, leading

tomuch more complex control requirements. On the other hand, this new circuit features a very simple voltage transfer ratio, given in (1), where *n* is the transformer turns ratio, and *D* is the duty cycle of the lower switch, Q_2 . Unlike the BHB, this transfer ratio is constant over both input load and frequency

—— =—— (1)

This voltage transfer ratio (1) is identical between the circuit shown in Figs. 2 and 3, indicating that only one pair of switches is necessary to provide controllability. Also, the transfer characteristic is similar to that of a CCM boost converter, simply multiplied by *n*. MPPT control of the CCM boost converter is widely discussed in the literature, with many different methods available such as perturb & observe (P&O) [8], ripple correlation control [9], and incremental conductance [10]. Also, several different control implementations are possible with theintegrated boost resonant (IBR) converter, such as input voltage [11], input current [12], and direct duty cycle control [13], giving tremendous control flexibility.

IV.CONVERTER OPERATION

The new topology can be effectively broken down into four distinct operating modes, shown in schematic form in Fig. 4(a)-(d) and as sections in the timing diagram provided in Fig. 5.

Mode I:

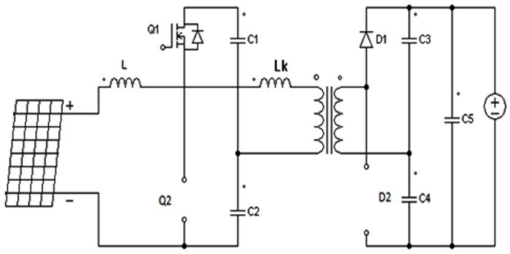

Fig. 4(a): Mode I of the proposed converter.

Beginning with the turnoff of Q2 prior to t_0, the current in the input inductor L flows into the body diode of Q1,discharging its parasitic capacitance. This allows Q1 to be turned ON under ZVS conditions at t0as in Fig.4(a). At this time, the upperinput-side capacitor C1 begins resonating with the transformer leakage inductance L_k and the output-side capacitors, C3 and C4, through D1.Simultaneously, the input current begins charging the series combination of C1 and C2. During this phase, Q1 carries the difference between the transformer current, flowing from C1 through thepositive terminal of the transformer and the input current. Once the transformer current resonates back to zero, D1 prevents the continued resonating in the reverse direction, ending mode 1.The length of the mode is given by:

$$Tres1=\pi \sqrt{\frac{[\quad)(\quad)]}{(\quad)}} \qquad (2)$$

Mode II:

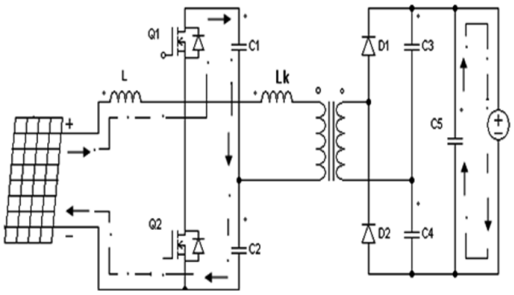

Fig.4(b): Mode II of the proposed converter

Q_1 is still active, yet it is only conducting the input inductor current, which is still decreasing, a pathway which is shown in Fig. 4(b). The resonant elements all conduct zero current during this interval. Only C_5 continuesdischarging into the load at this time. Mode 2 ends with the turn-off of Q_1 and the subsequent turn-on of Q_2

.

Mode III:

Fig.4(c): Mode III of the proposed converter.

After the turn-off of Q_1, but prior the turn-on of Q_2, the inductor current is still shunted into charging the series combination of C_1 andC_2 , thistime through the body diode of Q_1 , and still decreasing almostlinearly. When Q_2 is turned ON, the body diode of Q_1 is hard-commutated, causing some switching loss. Att_2 , C_2 begins to resonate with Lk and the parallel combination of C3 and C4,
through the diode D2 as in Fig.4(c). Simultaneously, the inductor current also flows through Q2, increasing linearly. During this interval, Q2 carries the sum of the transformer current and the inductor current. Thus, the rms current through Q2 is significantly larger than that of Q1,which carries the difference of the two currents. Once the transformer current resonates back to zero, D2 blocks the continued oscillation, marking the end of mode 3.

$$Tres2 = \sqrt{\frac{(\quad)}{(\quad)}} \qquad (3)$$

Mode IV

The inductor current continues to flow through the lower device, increasing until Q2 is turned OFF and the circuit returns to mode 1. Also, during both modes 3 and 4, Q1 effectively isolates the upper capacitor from charging

ordischarging. Note that there is a significant difference in the circuit behaviour between the two resonant modes (1 and 3). During mode 3, C1 is effectively isolated from the rest of the circuit due to the presence of Q1.Table1. Shows the values of power stage elements for the converter.

V. SIMULATION RESULTS

'Simulation' in general terms can be defined as the representation of a system in its realistic form.Before implementing a new project, by simulation, one can see the effect of various parameters or components on the output accordingly change them to get a desired output. PSIM denotes Power Simulation.PSIM is simulation software specifically designed for the analysis and design of power electronics and control circuits. It provides a powerful simulation and design environment for power supplies, analog/digital control and electric motor drives.Simview is the waveform display and post-processing program for PSIM. It provides a powerful environment to display and analyze simulation results. The circuit has been simulated at 40Vdc input by paralleling two solar panelsby using Psim Softwarefig6. demonstrate the consistency of the converter operation under high power, in this transformer current will retain their general wave shape while demonstrating CCM and Resonant behaviour respectively. To achieve the converter high efficiency, two other critical components were mentioned, mitigating switching lossand improving transformer power factor.Also, the fully resonant behavior at the transformer allows the converter to achieve a high power factor, as evidenced in Fig 6. One definitive aspectof managing the converter switching loss is the ability of the output diodes to achieve ZCS. Simulated evidence of this is provided in Fig.7

.

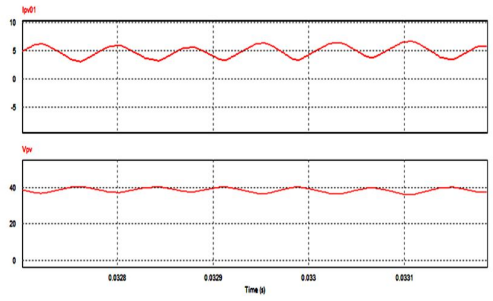

Fig 5:Key IBR converter operational waveform at 40vdc input.

Element	Value	Resistance	I_{rms} @ 250W
L	100µH	11mΩ	8.6A
C_1, C_2	10µF	4mΩ	11.46A, 6.64A
C_3, C_4	100nF	50mΩ	0.89A
C_5	2µF	N/A	N/A
$XFMR_{PRI}$	7 turns	3.5mΩ	12.84A
$XFMR_{SEC}$	46 turns	46mΩ	1.74A
Q_1	N/A	4.9mΩ	6.64A
Q_2	N/A	4.9mΩ	13.95A
D_1, D_2	1.3V	N/A	0.625A (Avg.)

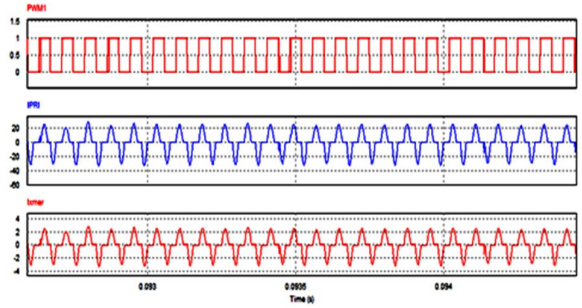

Fig 6: converter operational waveforms at 40vdc input and 250w/400vdc output

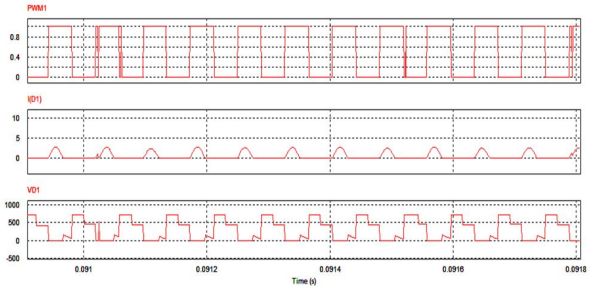

Fig 7: VGS and Output Diode ZCS at(40Vdc Input and 250w/ 400vdc output)

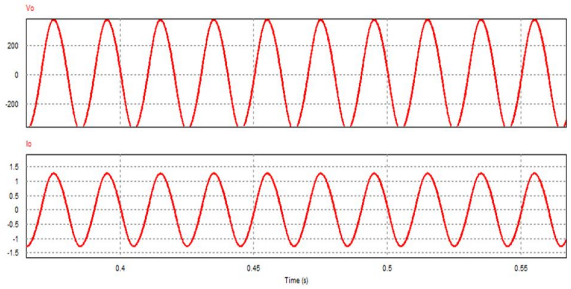

Fig 8: inverter stage output voltage and current waveforms

VI.CONCULSION

As a solution for providing efficient, distributed PV conversion, an isolated boost resonant converter has been proposed. The system is a hybrid between a traditional CCM boost converter and a series resonant half-bridge, employing only two active switches. The synthesis of the converter was described along with the circuit operating modes and key waveforms. The result was a simple process, requiring only consideration of the resonant period length in selecting a valid converter duty cycle range.

The principle advantages of utilizing this topology were as follows:

1. High weighted efficiency because of low circulating energy and reduced switching loss with resonant energy transfer and output diode ZCS.

2. Low potential cost due to minimal number of active devices and a small overall component count.

3. Galvanic isolation allows for the use of high efficiency inverter stages without additional concern over ground leakage current.

4. Reduced control complexity provides lower auxiliary power loss and simpler controller IC configurations.

Further efficiency improvements are possible with the addition of wide band gap semiconductor devices and passive component optimization.

REFERENCES

[1]A. S. Masoum, F. Padovan, and M. A. S. Masoum, "Impact of partial shading on voltage- and current-based maximum power point tracking ofsolar modules," in *Proc. IEEE PES General Meet.*, 2010,pp. 1-5.

[2] B. Brooks and C. Whitaker. (2005). *Guideline for the use of the Performance Test Protocol for Evaluating Inverters Used in Grid-Connected Photovoltaic Systems* [Online]. Available: http://www.gosolarcalifornia.org/equipment/documents/Sandia_Guideline_2005.pdf

[3] W.Bower, C.Whitaker, W.Erdman, M.Behnke, and M.Fitzgerald. (2004).*Performance Test Protocol for Evaluating InvertersUsed in Grid-Connected Photovoltaic Systems*

[4] O.Lopez, R. Teodorescu, F. Freijedo, and J. Doval Gandoy, "Leakage current evaluation of a single-phase transformerless PV inverter connectedto the grid," in *Proc. IEEE Appl. Power Electron. Conf.*, 2007, pp. 907-912.

[5] W. Yu, J.-S. Lai, H. Qian, and C. Hutchens, "High-efficiency MOSFET inverter with H6-type configuration for photovoltaic nonisolated ac-moduleapplications," *IEEE Trans. Power Electron.*, vol. 26, no. 4, pp. 1253-1260, Apr. 2011.

[6] T. Kerekes, R. Teodorescu, and U. Borup, "Transformer less photovoltaicinverters connected to the grid," in *Proc. IEEE Appl. Power Electron.Conf.*, 2007, pp. 1733-1737.

[7] Q.Li and P. Wolfs, "Recent development in the topologies for photovoltaicmodule integrated converters," in *Proc. IEEE Power Electron. Spec. Conf.*,2006, pp. 1-8.

[8]N. Femia, G. Petrone, G. Spagnuolo, and M. Vitelli, "Optimization ofperturb and observe maximum power point tracking method," *IEEE Trans.Power Electron.*, vol. 20, no. 4, pp. 963-973, Jul. 2005.

[9] T. Esram, J. W. Kimball, P. T. Krein, P. L. Chapman, and P. Midya"Dynamic maximum power point tracking of photovoltaic arrays usingripple correlation control," *IEEE Trans. Power Electron.*, vol. 21, no. 5, pp. 1282-1291, Sep. 2006.

[10] A. F. Boehringer, "Self-adapting dc converter for solar spacecraft powersupply," *IEEE Trans. Aerosp. Electron. Syst.*, vol. AES-4, no. 1, pp. 102-111, Jan. 1968.

[11] T.Tafticht and K. Agbossou, "Development of a MPPT method for photovoltaic systems," in *Proc. Can. Conf. Electr. Comput. Eng.*, 2004, vol. 2,pp. 1123-1126.

[12] J. A. Gow and C. D. Manning, "Controller arrangement for boost converter systems sourced from solar photovoltaic arrays or other maximum powersources," *IEE Proc.—Electr. Power Appl.*, vol. 147, no. 1, pp. 15-20, Jan2013.

[13] M. Veerachary, T. Senjyu, and K. Uezato, "Maximum power point tracking control of IDB converter supplied PV system," *IEE Proc.—Electr. PowerAppl.*, vol. 148, no. 6, pp. 494-502, Nov. 2001